1872 *Macromolecules* **1995,** *28,* 1872–1881

Viscoelastic and Dielectric Relaxation Behavior of Substituted Poly(*p*-phenylenes)

Michael Connolly and Frank Karasz*

Department of Polymer Science & Engineering, University of Massachusetts, Amherst, Massachusetts 01003

Mark Trimmer

Maxdem Incorporated, 140 East Arrow Highway, San Dimas, California 91773

Received November 8, 1994; Revised Manuscript Received January 4, 1995[⊗]

ABSTRACT: The thermal, dynamic mechanical, and dielectric relaxation behavior of poly(*p*-phenylenes) substituted with benzoyl and 4-phenoxybenzoyl groups and of a copolymer of benzoyl-1,4-phenylene and 1,3-phenylene were investigated. These amorphous materials were found to have flexural moduli higher than any other reported unoriented thermoplastic. Benzoyl-substituted poly(*p*-phenylene) which possesses the greatest rigid-rod character also displayed the highest modulus. The temperature dependence of viscoelastic and dielectric relaxation times were well described by the Williams–Landel–Ferry and Vogel–Fulcher equations, respectively. The temperature sensitivity or "fragility" of viscoelastic shift factors a_T and apparent dielectric relaxation times τ^* was greatest for the copolymer. The glass transition temperature of these polymers varied as a function of the total free volume. The polymer containing the 4-phenoxybenzoyl side group exhibited the lowest T_g due to internal plasticization, but the highest Vogel energy attributable to the large intramolecular bond rotational barrier associated with the bulky pendant group. The shape of frequency plane dielectric relaxation spectra of the substituted polyphenylenes could be accurately fitted to the Kolrausch–Williams–Watts (KWW) correlation function. The KWW stretched exponential term β displayed a very weak dependence on molecular structure and remained constant within experimental error for each material over the temperature range studied. Since β should be proportional to the degree of intermolecular coupling, the structural variation in "fragility", albeit small, of the substituted polyphenylenes may not be fully described by the coupling model for relaxation. Assuming the macroscopic expansion coefficient is proportional to the free volume expansion coefficient, the temperature dependence of τ^* and a_T may be explained more simply from free volume considerations. The 4-phenoxybenzoyl-substituted polymer displayed the highest expansion coefficient and largest total free volume, but the benzoyl-1,4-phenylene/1,3-phenylene copolymer exhibited the largest relative change in free volume with temperature, which explained the greater "fragility" of the copolymer compared to either homopolymer.

I. Introduction

Engineering thermoplastics continue to find new applications and often replace traditional structural materials of metal and ceramic. It is empirically observed that incorporation of a large fraction of main chain aromatic groups in a polymer imparts high temperature stability. Unfortunately, the aromatic nature of polymers such as poly(*p*-phenylene) results in highly crystalline, insoluble, and infusible materials which are thereby excluded from use in structural applications.

To optimally balance material performance and processing characteristics, research groups have studied systems which incorporated side chains on linear aromatic polymers including poly(*p*-phenylene).[1-4] Recently, Marrocco and co-workers[5-7] have reported large-scale synthesis of high molecular weight substituted polyphenylenes. They observed unusually high flexural moduli (approximately 10 GPa) for materials which were thermoplastic, remained soluble in common organic solvents after processing, and displayed no crystallinity detectable by DSC or X-ray analysis.

In this contribution, we report on the thermal, dynamic mechanical, and dielectric relaxation behavior of poly(1,4-phenylenes) substituted with either benzoyl or 4-phenoxybenzoyl groups and a copolymer of benzoyl-1,4-phenylene with 1,3-phenylene in order to more fully understand their basic properties. We are interested particularly in the nature of segmental motions which are responsible for the glass to rubber transition. In linear flexible and semiflexible polymers, the glass transition represents the onset of long range diffusive motions of chain backbone segments. The molecular structure of the repeat units controls this segmental motion. Polymers which contain small, flexible repeat units such as poly(oxymethylene) are limited in their segmental motion primarily by local bond rotational barriers and hence display symmetric, Debye-type relaxation spectra and a near-Arrhenius temperature dependence of their relaxation times. Conversely, polymers with large, sterically hindered monomer segments such as Bisphenol A polycarbonate (BPA-PC) exhibit very broad, asymmetric relaxation spectra with relaxations times having a distinctly non-Arrhenius temperature dependence. Ngai and co-workers[8-10] have attributed these effects of chemical structure to the *inter*molecular cooperativity or coupling of segmental motions with relaxations of neighboring, nonbonded segments. The rigid-rod nature of substituted polyphenylenes studied in this report provides an interesting new topology for evaluation of the concepts of the cooperativity model.

II. Experimental Section

A. Materials. The benzoyl- and 4-phenoxybenzoyl-substituted poly(*p*-phenylenes) were supplied by Maxdem, Inc. (PX-1000 and PX-2000, respectively) together with an experimental

---

* To whom correspondence should be addressed.

[⊗] Abstract published in *Advance ACS Abstracts,* February 15, 1995.

0024-9297/95/2228-1872$09.00/0

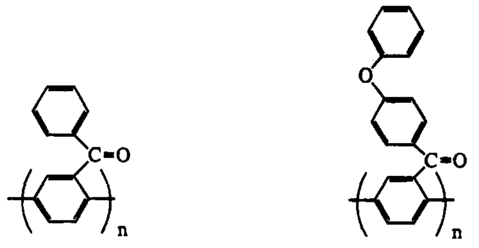

PX™-1000
Poly(benzoyl-1,4-phenylene)

PX™-2000
Poly(4'-phenoxybenzoyl-1,4-phenylene)

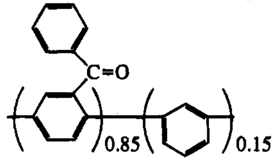

P-1
Poly[(benzoyl-1,4-phenylene)-*co*-1,3-phenylene]

Figure 1. Structures of Poly-X polyphenylenes.

Table 1. Characterization of Poly-X Poly(*p*-phenylenes)

	calculated wt %		measured wt %	
sample	C	H	C	H
PX-1000	86.68	4.44	87.10	4.53
PX-2000	83.83	4.41	83.99	4.41
P-1	87.24	4.50	87.97	4.51

85/15 (mol/mol %) benzoyl-1,4-phenylene/1,3-phenylene copolymer (**P-1**). The chemical structure of each material (Figure 1) was confirmed by elemental analysis and IR spectroscopy. Elemental analysis results (University of Massachusetts Microanalytical Laboratory) are reported in Table 1. The as-received powders were redissolved in chloroform (5 wt %) over a 24 h time period using mild heating and vigorous stirring. Samples were precipitated by slowly pouring the pale yellow chloroform solutions into a high-speed blender containing a 10-fold excess of methanol. The precipitate was collected in a fritted glass funnel, dried in vacuum for 12 h at room temperature, 24 h at 80 °C, and finally at 120 °C for 12 h, and stored *in vacuo*. Bisphenol A polycarbonate (BPA-PC) pellets were used as-received (Aldrich). The weight average molecular weight (M_w) of the BPA-PC was found to be 21 800 by static light scattering in THF at 25 °C compared to a polystyrene calibrated GPC value of M_w = 47 000, and molecular weight distribution (MWD) = 2.30 in THF at 30 °C.

Samples were prepared for analysis by compression molding in vacuum at 300 °C under approximately 3 metric tons of pressure. Powder samples of the Poly-X resins were initially sintered into solid slabs by placing the powder between Kapton sheets and compressing at 300 °C for 30 s under 1 metric ton pressure. Samples for dynamic mechanical analysis were formed by molding the sintered powders into rectangular bars 1 mm thick, 10 mm wide, and 30 mm long. To ensure formation of uniform and reproducible specimens, material placed between Kapton sheets was held in vacuum at 300 °C for 5 min before applying pressure to achieve thermal equilibrium, annealed a further 15 min after molding to allow the sample to relax, and then cooled to 50 °C over a period of 10 min before removing from the vacuum chamber. Dielectric samples approximately 0.3 mm thick and 33 mm in diameter were prepared directly from the dry precipitate by placing approximately 0.3 g of polymer between Kapton sheets in a pellet type mold. Disks for dielectric analysis were molded under the same conditions as described for the dynamic mechanical samples, although 12 min was allowed for initial thermal equilibration due to the greater thermal mass of the mold. All samples remained soluble after compression molding.

BPA-PC samples were molded at 200 °C by compressing the as-received pellets into the desired mold using the same thermal equilibration method as used for the Poly-X resins.

B. Instrumental Methods. Sample degradation temperature and residual solvent content of the precipitated powders were determined using a Perkin-Elmer System 7 thermogravimetric analyzer (PE-TGA7). TGA experiments were performed on samples between 7 and 12 mg at 20 °C/min under a dry nitrogen atmosphere from 30 to 900 °C. All poly(*p*-phenylenes) studied exhibited less than 0.5% weight loss up to 300 °C, and this can be attributed to residual solvent and adsorbed water. Under dry N_2, 60–80 wt % char of the Poly-X resins remained at 900 °C. Expansion coefficient measurements were obtained on a DuPont 2940 thermomechanical analyzer (TMA), calibrated with indium using a 2.54 mm diameter expansion probe under a 0.05 N load. Samples approximately 1 mm thick were tested at 10 °C/min under dry N_2 from 50 to 200 °C after cooling from 200 °C at 10 °C/min. The glass transition temperature (T_g) was defined as the onset of the slope change in the expansion curves.

Dynamic mechanical experiments were performed under dry nitrogen on a Polymer Laboratories DMTA Mk I in the single cantilever bending mode. Samples with a free length of 8 mm were constrained using a 0.30 Nm torque on each clamp nut. Thermal scans were made from −100 to +250 °C at 2 °C/min at 1, 3, 10, and 30 Hz. Isothermal measurements were made at six frequencies between 0.1 and 30 Hz in 5 deg steps after allowing 6 min for the sample to reach thermal equilibrium.

Dielectric relaxation behavior was measured on a GenRad 1689M Digibridge which was interfaced with a Polymer Laboratories DETA Mk I system using an unguarded parallel plate cell of 31 mm diameter. Samples were sputter coated with gold and studied in thermal scans from −100 to +250 °C at 2 °C/min at 0.2, 1, 10, 28.5, and 100 kHz. Isothermal experiments were performed at 35 frequencies between 20 Hz and 100 kHz using 2–5 deg temperature intervals and 10 min thermal equilibration.

Solutions of the copolymer (**P-1**) possessed much lower viscosities (η_{inh} = 1.1 dL/g at 40 °C in 0.05 M LiBr/NMP using a Cannon-Ubbelodhe viscometer and a solution concentration of 0.10 g/dL) than the benzoyl- and 4-phenoxybenzoyl-substituted polymers (PX-1000 and PX-2000, respectively). To ensure that the low viscosity of **P-1** was due only to the flexible nature of the *m*-phenylene kink units, the M_w of **P-1** was determined by static light scattering using an Otsuka Electronics DLS-700 spectrophotometer which was calibrated with benzene (Aldrich Chemical Co., 99.9% HPLC grade) using a Rayleigh ratio[11] of 12.63×10^{-3} cm^{-1}. Samples were dissolved in chloroform (Aldrich Chemical Co., 99.8% ACS spectrophotometric grade) at four concentrations between 1 and 5 mg/mL and were filtered five times to remove dust using 0.22 μm Millipore FGS filters. All solvents were used as-received from the manufacturer. The refractive index increment with concentration (d*n*/d*c*) of the **P-1** light scattering solutions was measured using an Otsuka Electronics RM-102 differential refractometer using a Brice-type split cell. Using a d*n*/d*c* of 0.2628 ± 0.004 at 25 °C, the M_w of **P-1** using a Zimm plot extrapolation was found to be 26 900 ± 1000, indicating a weight average degree of polymerization of 164 ± 6. The high viscosities of the homopolymer solutions precluded a meaningful M_w measurement with available instrumentation.

All Vogel–Fulcher and WLF fits of temperature dependent relaxation behavior were made using Kaleidagraph 3.0 graphics software (Abelbeck Software Inc.). The Kolrausch–Williams–Watts parameters $\Delta\epsilon$ and β were determined by comparing the shape of normalized dielectric loss spectra ($\epsilon''/\epsilon''_{max}$) to the related probability density functions.[12,13] The latter were calculated using a UNIX-based program provided by the General Electric Co. Before analyzing the dielectric relaxation curves, the conductivity contribution ϵ''_{cond} to the loss was subtracted from the low-frequency side of the spectrum assuming $\epsilon''_{total} = \epsilon''_{dipolar} + \epsilon''_{cond}$ and $\epsilon''_{cond} = (2\pi fRC_0)^{-1}$ where *f* is the measurement frequency, *R* is the dc resistance, and C_0 is capacitance of an air gap equal to the sample thickness.

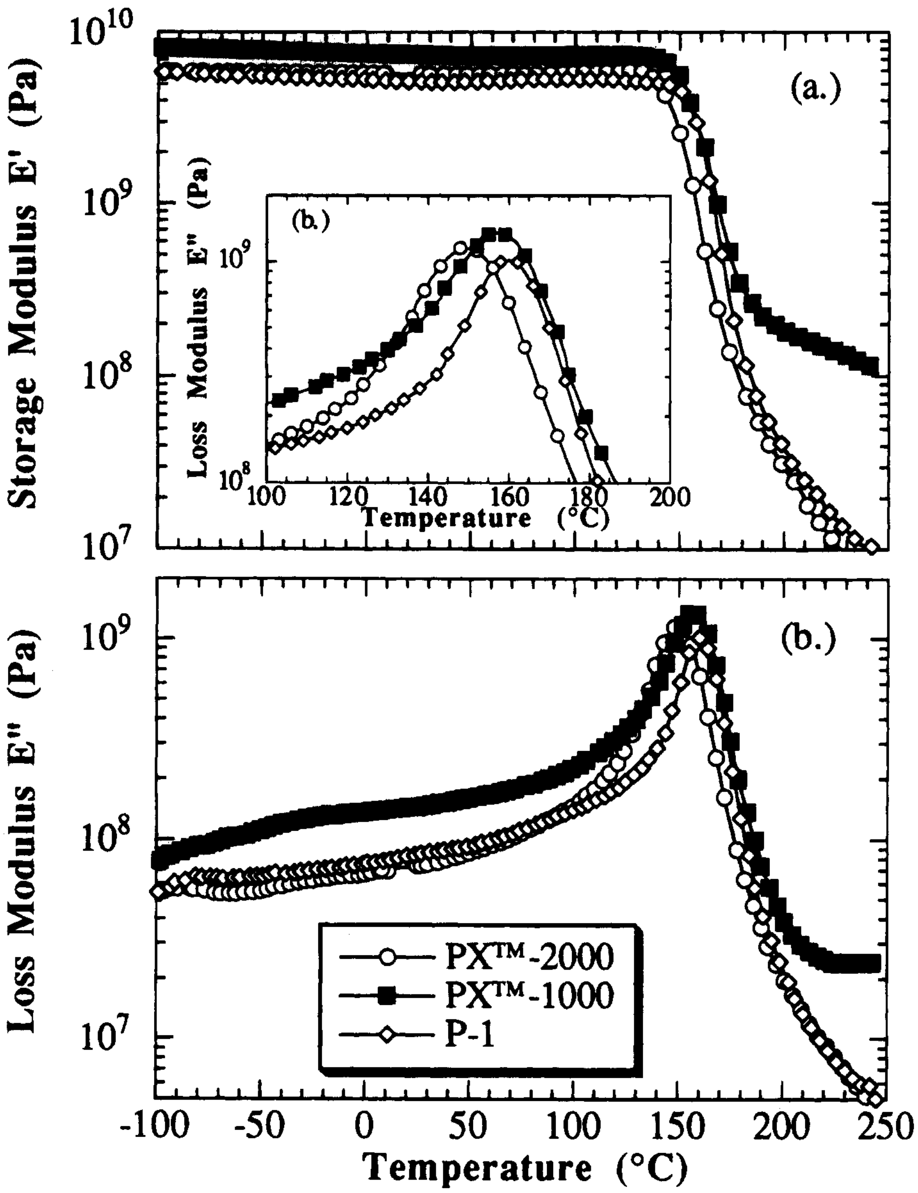

Figure 2. Temperature dependence of (a) storage E' and (b) loss E'' moduli at 10 Hz for Poly-X polyphenylenes.

III. Results and Discussion

The dynamic mechanical behavior of the Poly-X resins over a wide temperature range is shown in Figure 2. The glassy moduli of these materials were found to be higher than any other reported amorphous thermoplastic. Storage moduli (E') of 5.2, 6.0, and 7.6 GPa at 25 °C and 10 Hz for **P-1**, PX-2000, and PX-1000, respectively, agree well with the static flexural moduli of between 7 and 10 GPa reported previously.[6,7] These values may be compared to the flexural moduli of the amorphous engineering thermoplastics BPA-PC and BPA-polysulfone, 2.3 and 2.7 GPa, respectively. The rodlike polyphenylene backbone is capable of supporting large mechanical stresses, resulting in very high moduli even though these polymers are unoriented and noncrystalline. As expected, PX-1000 which possesses the greatest rigid-rod character exhibits the highest modulus while **P-1** which contains nonlinear, "kink", units has the lowest modulus and highest ductility.[6,7] It should be noted that the dynamic modulus described here is somewhat lower than that obtained in static flexural tests due to the relatively small sample size and finite instrumental compliance; the reproducibility of the DMTA modulus measurements is better than ±1 GPa.

The glass transition temperature (T_g) of the polyphenylenes varies slightly with the substituent. PX-2000 which contains the largest side groups displays the lowest T_g of 150 °C, compared to 158 and 161 °C for PX-1000 and **P-1**, respectively. We expected initially that **P-1** would possess the greatest mobility and lowest T_g since it incorporates *m*-phenylene units, disrupting the rigid-rod character of the *p*-phenylene backbone. Apparently, the large free volume induced by the bulky benzoyl and 4-phenoxybenzoyl side groups largely controls the segmental mobility of these polyphenylenes. As has been observed in alkyl methacrylate polymers, for example, increasing side-chain length results in an increase in free volume and a decrease of T_g. There appears to be little effect of the side group on the subambient mechanical relaxation behavior of the Poly-X materials. Only a very broad, weak relaxation is observed for all three polymers between −100 and +50 °C, indicating either that the side groups have restricted mobility in the glassy state or that the local relaxation modes do not significantly damp mechanical oscillations.

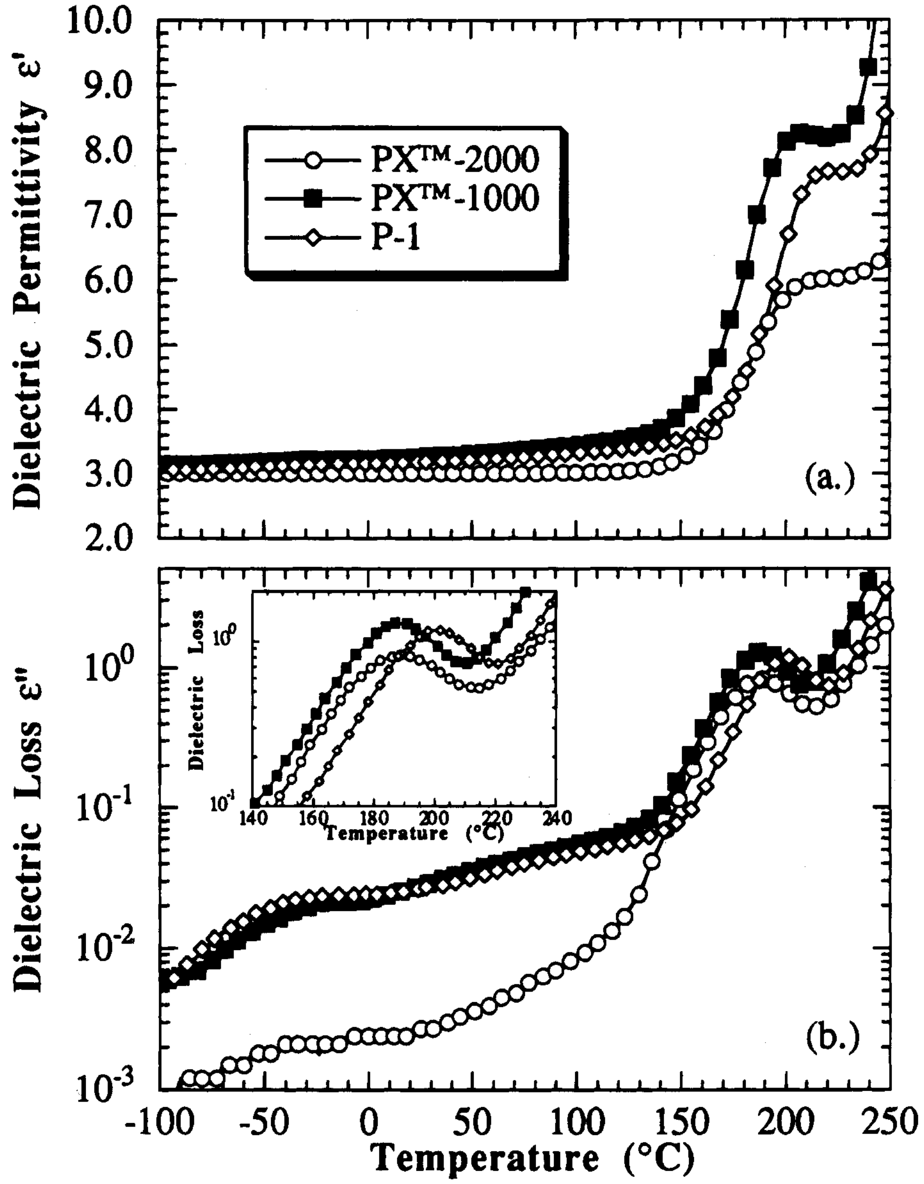

Figure 3. Temperature dependence of (a) dielectric permittivity ϵ' and (b) dielectric loss ϵ'' at 10 kHz for Poly-X polyphenylenes.

As shown in Figure 3, a similar T_g trend was observed in the dielectric measurements of the substituted polyphenylenes; *i.e.*, **P-1** displays the highest T_g. Polymers such as poly(methyl methacryate) (PMMA) which contain strong dipoles in the side group typically also exhibit very strong local mode dielectric relaxations. PMMA shows only a weak mechanical β relaxation, but the magnitude of the dielectric β relaxation exceeds that of the T_g or α relaxation. In the polyphenylene family studied here, the strong dipoles of the benzoyl and 4-phenoxybenzoyl groups have only limited mobility in the glassy state; these materials display only weak local mode relaxations in the vicinity of −50 °C. The dipole moments of PX-1000 and PX-2000 repeat units are approximately equivalent to those of benzophenone ($\mu = 2.98$ D) and 4-phenoxybenzophenone ($\mu \approx 1.82$ D).[14] In the copolymer **P-1**, the average dipole moment may be regarded as the weighted average of benzophenone and benzene which has no dipole moment. Considering these approximations, the dielectric permittivity ϵ' and relaxation strength $\Delta\epsilon$ (the difference in ϵ' above and below T_g) of each of the Poly-X materials correlate with the strength and number of their respective polar side groups.

To more thoroughly probe the dynamics of these substituted polyphenylenes, the temperature dependence of the dynamic mechanical and dielectric relaxation spectra was determined using measurement conditions outlined above. For a system possessing a single relaxation mechanism, the temperature dependence of viscoelastic relaxation times has been described by the empirical Williams–Landel–Ferry (WLF) equation:[15,16]

$$\log a_{\mathrm{T}} = \log\left(\frac{\tau^*}{\tau_{\mathrm{R}}^*}\right) = \frac{-C_1(T - T_{\mathrm{R}})}{C_2 + T - T_{\mathrm{R}}} \qquad (1)$$

where a_{T} is the WLF shift factor, τ^* is the apparent relaxation time at temperature T and is defined as $1/(2\pi f_{\max})$ with $f_{\max}$ equal to the frequency of the mechanical loss (E'') peak, τ_{R}^* is the apparent relaxation time at the reference temperature T_{R}, and C_1 and C_2 are the WLF constants equal to $B'/2.303f_{\mathrm{R}}$ and f_{R}/α_f, respectively. B' is the Doolittle parameter on the order of unity, f_{R} is the fractional free volume at T_{R}, and α_f is the thermal expansion coefficient of the fractional free volume. The temperature dependence of the WLF shift factor a_{T} is plotted in Figure 4 for each of the polyphenylene resins and the fit of each curve to the WLF

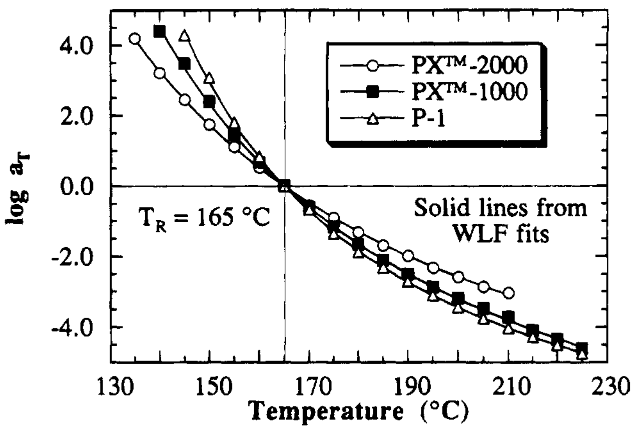

Figure 4. WLF plot of viscoelastic shift factors a_T for all Poly-X resins.

Table 2. WLF Parameters for Poly-X Mechanical Relaxation Behavior[a]

sample	C_1	C_2 (K)	T_R (°C)	R
PX-2000	10.2 ± 0.1	103.1 ± 1.4	165	0.9999
PX-1000	11.2 ± 0.2	88.6 ± 1.4	165	0.9998
P-1	9.9 ± 0.1	65.1 ± 0.7	165	0.9999

[a] Determined by fitting the Williams–Landel–Ferry equation (eq 1) to the data in Figure 4.

equation (eq 1) is recorded in Table 2. It is clear that PX-2000 exhibits a weaker temperature dependence of its relaxation time than either PX-1000 or **P-1**. The nature of this dependence will be discussed below.

An alternative empirical expression describing the temperature dependence of relaxation times was introduced by Vogel[17] and Fulcher:[18]

$$\log \tau^* = \log \tau_0 + \frac{E}{2.303R(T - T_0)} \qquad (2)$$

where τ^* is the apparent relaxation time at temperature T from the mechanical (E'') or dielectric (ϵ'') loss maximum, τ_0 is the primitive relaxation time at the Vogel temperature T_0 where the system entropy approaches zero, and E is an energy term of the order of bond rotational barriers. The Vogel–Fulcher equation has been used successfully in studies[9,19–22] to describe the temperature dependence of dielectric and mechanical relaxation times of homopolymers as well as of polymer blends and solutions. The apparent relaxation times τ^* of the substituted polyphenylenes from dielectric frequency plane measurements are presented in Figure 5 in an Arrhenius-type plot together with the best fits to the Vogel–Fulcher equation. The behavior of BPA-PC which is known to have high intramolecular bond rotational barriers is also plotted in Figure 5 for comparison. The Vogel–Fulcher parameters of the best fit curves in Figure 5 are listed in Table 3. Although it exhibits the lowest T_g and hence the lowest T_0 of the three polyphenylenes, PX-2000 displays the highest Vogel energy E. Considering the size of the 4-phenoxybenzoyl group compared to a benzoyl group, it would be expected that the bond rotational barrier around the main chain phenylene segment in PX-2000 would be larger than PX-1000 or **P-1**.

The WLF constants C_1 and C_2 at T_R obtained from viscoelastic measurements may be recalculated for the glass transition temperature T_g obtained from volumetric or calorimetric measurements:[23]

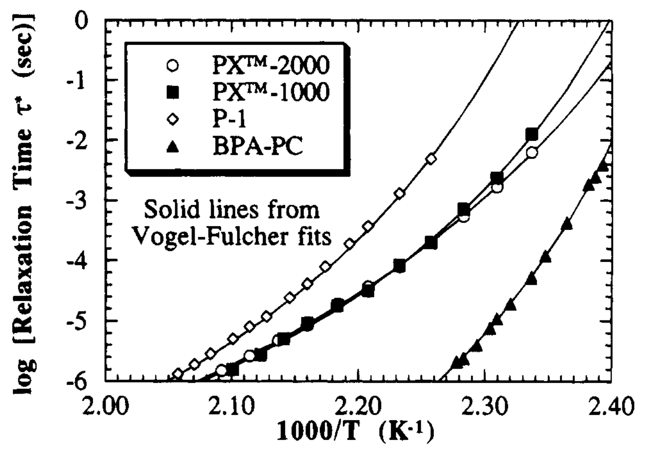

Figure 5. Arrhenius plot of apparent dielectric relaxation times τ^* for the α-relaxation of Poly-X resins.

Table 3. Vogel–Fulcher Parameters for Poly-X Dielectric Relaxation Behavior

sample	log τ_0[a] (s)	E[a] (kJ/mol)	T_0[a] (°C)	R	T_g ($\tau^* = 1$ s)[b] (°C)
PX-2000	−11.6 ± 0.3	14.3 ± 1.2	74.8 ± 4.0	0.9999	140
PX-1000	−10.8 ± 0.6	10.6 ± 1.8	92.6 ± 6.7	0.9993	144
P-1	−11.5 ± 0.4	11.8 ± 1.4	104.0 ± 4.9	0.9996	157
BPA-PC	−12.9 ± 0.8	9.0 ● 1.7	100.2 ± 4.8	0.9995	139

[a] Determined by fitting the Vogel–Fulcher equation (eq 2) to the data in Figure 5. [b] Calculated from the Vogel–Fulcher equation using the parameters listed above.

$$C_1 = \frac{C_{1g}C_{2g}}{C_{2g} + T_R - T_g} \qquad (3a)$$

$$C_2 = C_{2g} + T_R - T_g \qquad (3b)$$

where C_{1g} and C_{2g} are the new WLF constants at T_g. Using the observation that $T_0 = T_g - C_{2g}$, the WLF equation can be rewritten to include the Vogel temperature:

$$\log a_T = \frac{C_{1g}(T - T_g)}{(T - T_0)} \qquad (4)$$

Therefore, by definition, the WLF shift factor a_T diverges to infinity when $T = T_0$. The apparent activation energy (E_a) of a viscoelastic relaxation follows a distinctly non-Arrhenius temperature dependence:[23]

$$E_a = \frac{2.303RC_{1g}C_{2g}T^2}{(C_{2g} + T - T_g)^2} \qquad (5a)$$

or

$$E_a(T_g) = \frac{2.303RC_{1g}(T_g)^2}{C_{2g}} \qquad (5b)$$

at $T = T_g$. Since at high temperatures each molecular segment relaxes independently, the primitive activation energy E associated with local bond rotational barriers is

$$E = 2.303RC_{1g}C_{2g} \qquad (5c)$$

equivalent to the activation energy of noncooperative intramolecular bond rotation $\Delta\mu^*$ used by Matsuoka[24] where $\Delta\mu^*/k = 1/\alpha_f$.

Table 4. WLF and Vogel–Fulcher Parameters at T_g for Poly-X Mechanical Relaxation Behavior

sample	T_g[a] (°C) (±0.5)	10^{-4} $\Delta\alpha$[a] (°C^{-1}) (±0.15)	C_{1g}[b] (±0.6)	C_{2g}[b] (K) (±1.8)	T_0[c] (°C) (±2.5)	E[c] (kJ/mol) (±1.3)	$E_a(T_g)$[d] (kJ/mol) (±35)
PX-2000	156.5	5.15	11.1	94.6	61.9	20.1	414
PX-1000	159.2	3.09	11.9	82.8	76.4	18.9	514
P-1	160.7	2.33	10.5	60.8	99.9	12.3	622

[a] Measured by TMA at 10 °C/min [$\Delta\alpha = \alpha(\text{liquid}) - \alpha(\text{glass})$]. [b] Calculated from eqs 3a and 3b. [c] $T_0 = T_g - C_{2g}$ and $E = 2.303RC_{1g}C_{2g}$ (eq 5c). [d] Calculated from eq 5b using T_g by TMA.

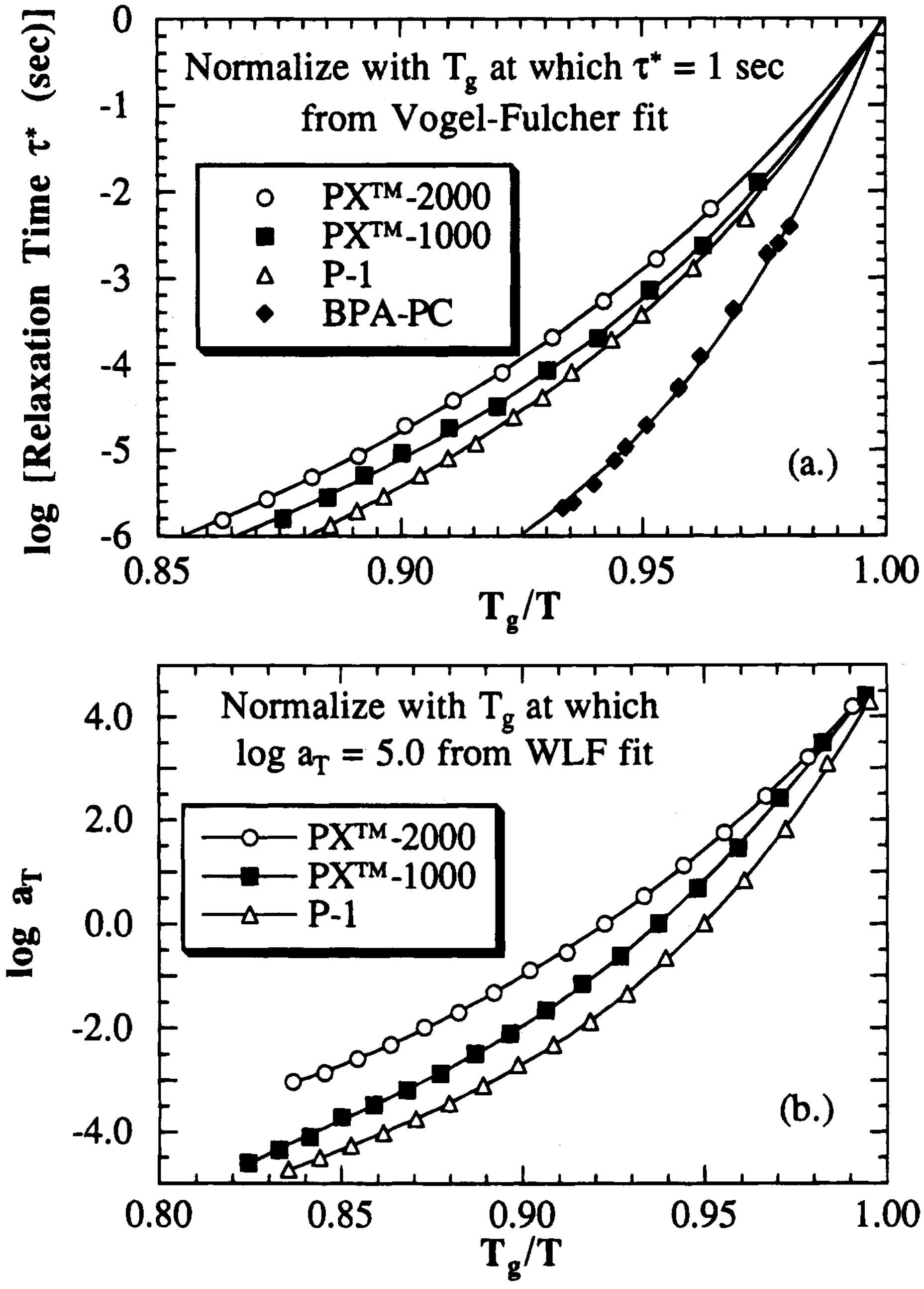

Figure 6. Cooperativity plot of (a) dielectric relaxation times τ^* and (b) WLF shift factors a_T for Poly-X polyphenylenes.

Using eqs 3–5, T_0, E, and $E_a(T_g)$ were calculated (Table 4) for each of the Poly-X polyphenylenes from the WLF parameters in Table 2. Although there are quantitative differences between both the Vogel energies and the Vogel temperatures (Tables 3 and 4), a consistent trend is observed. PX-2000 exhibits the highest intramolecular bond rotational barrier and lowest T_0 while **P-1** displays the lowest Vogel energy and highest T_0. The differences between the viscoelastic and dielectric Vogel parameters may be explained by the different domain sizes of the experimental probes. Since dielectric measurements examine the mobility of dipolar molecular segments, the experimental domain size is on the order of monomer units while viscoelastic experiments reveal relaxations of 5–10 repeat units. Ngai[19] has discussed the correlation between viscoelastic, dielectric, and dynamic light scattering relaxation times in this manner.

The effect of molecular structure on the temperature dependence of relaxation times is not obvious from the shift factor or τ^* data (Figures 4 and 5). Roland and co-workers[8–10,21] have attempted to show that a correlation exists between the shape of the viscoelastic or dielectric relaxation spectrum and the temperature

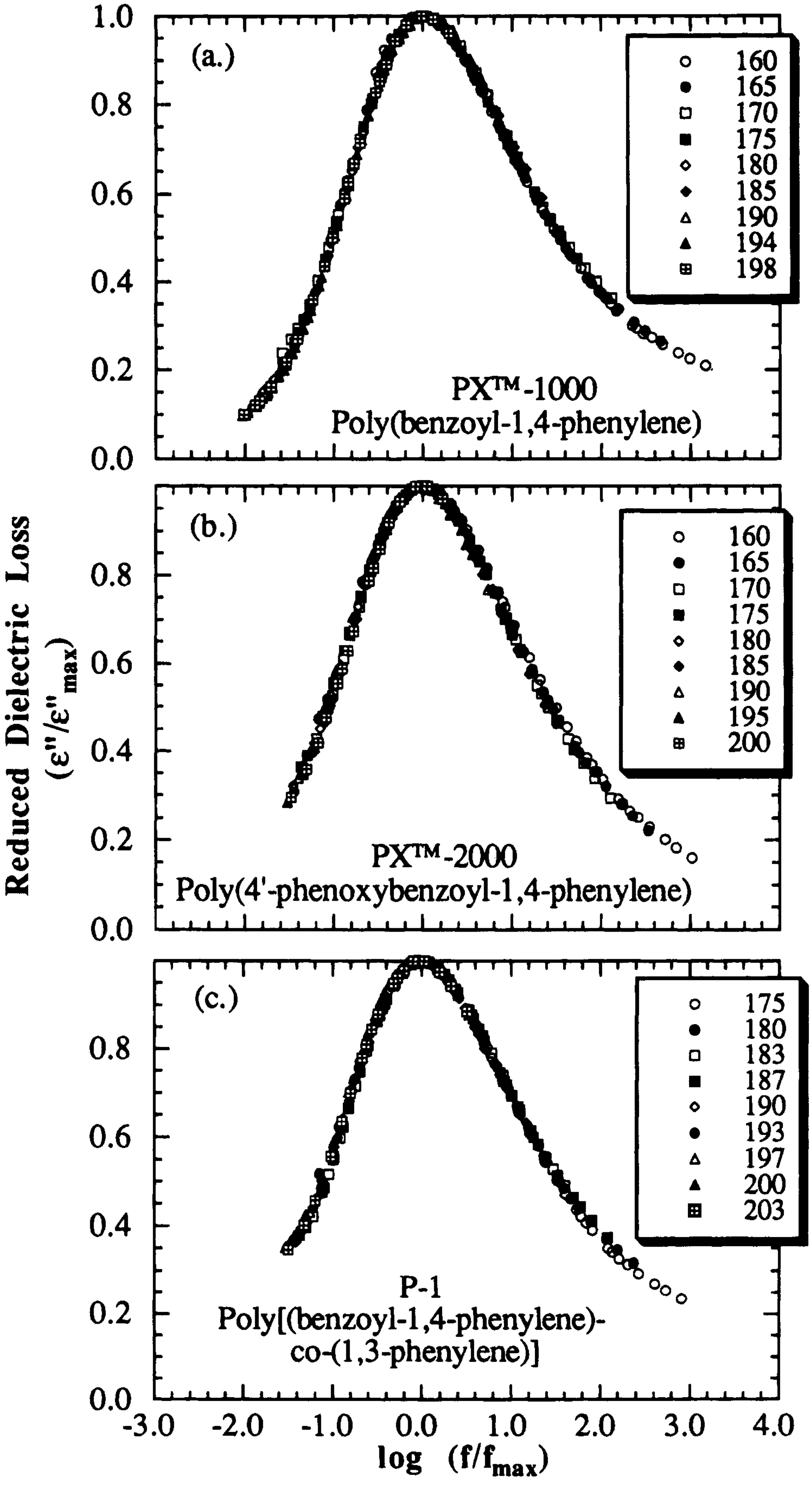

Figure 7. Reduced dielectric loss ($\epsilon''/\epsilon''_{\max}$) mastercurves for (a) PX-1000, (b) PX-2000, and (c) **P-1** where $f_{\max}$ is the frequency at the dielectric loss maximum $\epsilon''_{\max}$.

dependence of relaxation times. In their coupling model of relaxation, Roland and co-workers have proposed that τ^* is determined not only by the local friction coefficient (as in free volume concepts of relaxation) but also by the extent of intermolecular cooperative rearrangements. Angell[25] introduced the convenient representa-

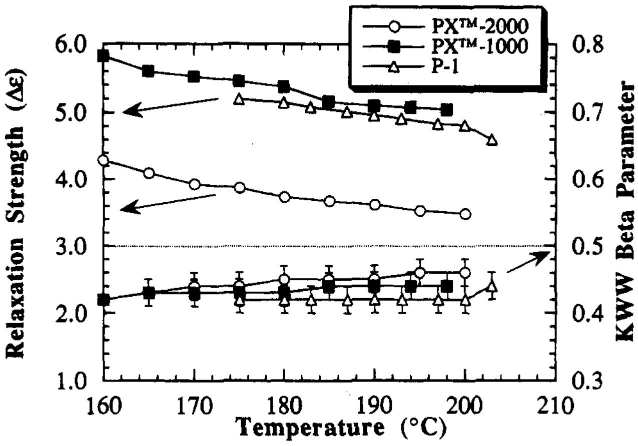

Figure 8. Temperature dependence of Poly-X dielectric relaxation strength $\Delta\epsilon$ and KWW stretched exponential parameter β.

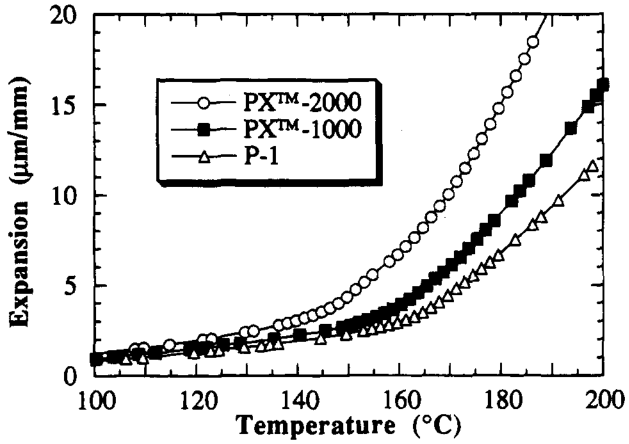

Figure 9. Thermal expansion curves of Poly-X resins.

tion of a_T or τ^* data in terms of a normalized temperature T_g/T using an arbitrary glass transition temperature T_g outside the measurement range to scale the data appropriately. In such "fragility" or "cooperativity" plots, materials which exhibit greater temperature sensitivity of a_T or τ^* will possess a greater degree of intermolecular cooperative motion. The experimental shift factor and dielectric relaxation data for the three polyphenylenes are replotted in Figure 6 in the form of a cooperativity plot. As suggested by the fits of this data to the Vogel–Fulcher and WLF equations discussed earlier, the viscoelastic and dielectric relaxation times possess a similar temperature dependence. This observation implies that both methods examine the same relaxation mechanism, albeit on a different length scale. These cooperativity plots also suggest that the degree of intermolecular cooperative motion is greatest in **P-1** since it displays the most pronounced temperature sensitivity of a_T and τ^*.

To examine more closely the nature of cooperative motion in the Poly-X resins, we have analyzed the shape of the dielectric relaxation spectrum. Many studies have proved that the empirical Kolrausch–Williams–Watts (KWW) equation:[26]

$$\phi(t) = \exp(-t/\tau^*)^{\beta} \qquad 0 \le \beta \le 1 \tag{6}$$

can be used to accurately fit the dielectric and mechanical loss spectra of many polymers in the vicinity of the glass transition temperature. In this expression, $\phi(t)$ is the dipole moment correlation function, τ^* is the temperature-dependent relaxation time, and β is the "stretched" exponential factor which indicates the distribution of relaxation times. When $\beta = 1$, eq 6 represents a simple Debye-type relaxation. In the coupling model of Roland *et al.*,[9,10,21] the KWW β parameter is equal to $1 - n$ where n represents the coupling parameter and is said to indicate the strength of intermolecular cooperative rearrangements. Hence, the relaxation spectrum will broaden as the coupling parameter increases. Weiss and co-workers[12,13] have expressed the dielectric loss function as

$$\epsilon''(\omega) = \Delta\epsilon \cdot z \cdot Q_{\alpha}(z) \tag{7a}$$

with

$$Q_{\alpha}(z) = \frac{1}{\pi}\int_0^{\infty} \exp(-u)^{\beta} \cos(zu)\, \mathrm{d}u \tag{7b}$$

where $\Delta\epsilon$ is the dielectric relaxation strength, $z = \omega\tau^*$, and $\omega = 2\pi f$. They have developed a computational method to solve the "stable" probability density function $Q_\alpha(z)$ over a wide range of β and z. Using this algorithm, we have calculated $\Delta\epsilon$ and β for the Poly-X polyphenylenes.

The normalized dielectric loss spectrum of each of the Poly-X polyphenylenes over a wide temperature range is plotted versus normalized frequency in Figure 7. Comparing the three data sets, there appears to be little variation in the KWW factor β at any temperature since the shapes of the loss curves are almost identical. The relaxation strength $\Delta\epsilon$ and KWW factor β for each sample and at all temperatures have been plotted in Figure 8. According to Frölich[27]

$$\Delta\epsilon \propto \mu_e^{\,2}/T \tag{8}$$

where μ_e is the effective dipole moment per repeat unit. As expected, the relaxation strength for each sample was found to be inversely proportional to temperature and the relative magnitude of $\Delta\epsilon$ varied according to the dipole moment of the repeat unit, as seen in the thermal scans of the substituted polyphenylenes. Within the experimental error of ±0.02, the stretched exponential term β was nearly constant over the temperature range studied. Only a very weak dependence of β on the chemical structure of the polyphenylene was observed. Since β varies only from 0.42 to 0.46 over all temperatures and structures, the corresponding coupling parameter ($n = 1 - \beta$) varies in the narrow range from 0.54 to 0.58. As discussed previously, an increase in the "fragility", *i.e.*, the temperature dependence of the relaxation times, should be accompanied by a corresponding increase of intermolecular coupling. For example, in a homologous series of polybutadienes, Roland and Ngai[9] concluded that the content of vinyl groups correlated with the broadening of the viscoelastic relaxation spectra, *i.e.*, the increase of intermolecular coupling and with the "fragility" of the polymers. Since the coupling parameter n varied only slightly in this study with molecular structure, the temperature dependence of relaxation times for the Poly-X polyphenylenes may not be fully explained by the coupling model.

The free volume theory is a straightforward approach which has been used more often than the coupling model to describe segmental relaxation dynamics. From this perspective, the molecular mobility at any temperature is controlled by the free volume or the unoccupied

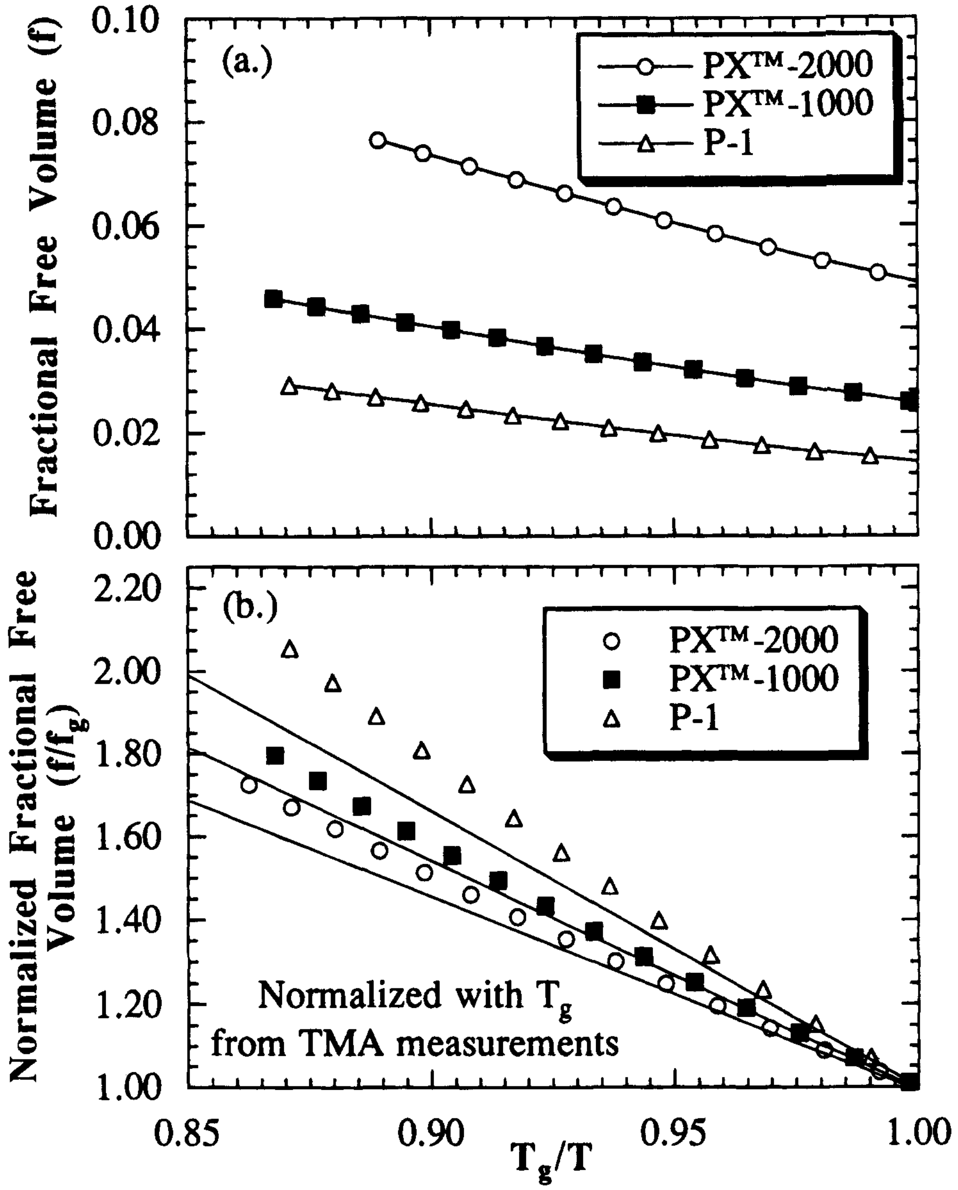

Figure 10. (a) Fractional free volume f and (b) normalized fractional free volume f/f_g versus reduced temperature for Poly-X polyphenylenes. (The straight lines represent the initial slope of the normalized free volume.)

volume between chains. The onset of a glass transition is determined by a reduction in the rate of free volume collapse as the temperature is lowered. The traditionally vague concept of fractional free volume f has been defined as V_f/V_g where V_f and V_g are the free volumes at any temperature T and T_g, respectively. Ferry[23] has assumed that the fractional free volume increases linearly with temperature as

$$f = f_g + \alpha_f(T - T_g) \qquad (9a)$$

However, neither f nor α_f may be determined by direct experimental methods. Assuming that α_f equals $\Delta\alpha$, the difference between the macroscopic expansion coefficients of the liquid α_l and glassy α_g states,[28-30] the fractional free volume at $T_g(f_g)$ and f may be calculated as follows:

$$f_g = C_{2g}\Delta\alpha \qquad (9b)$$

and

$$f = \Delta\alpha(C_{2g} + T - T_g) \qquad (9c)$$

The thermal expansion curves for the substituted polyphenylenes are shown in Figure 9. Although the expansion coefficients in the glassy state are similar, PX-2000 clearly exhibits a much higher value of α_l than PX-1000 or **P-1**. On the basis of eq 9b, the fractional free volume at T_g of PX-2000 was found to be twice that of PX-1000 and more than 3 times that of **P-1**. Since T_g is inversely proportional to free volume, this observation is consistent with the dynamic mechanical and dielectric thermal scans at fixed frequency discussed above in which the T_g increased from PX-2000 to PX-1000 to **P-1**. When viewed in a normalized temperature format (Figure 10a), the rate of free volume expansion with temperature is greatest for PX-2000 and smallest for **P-1**. Considering only the total free volume, it might be expected that PX-2000 would display the greatest "fragility" of these polyphenylenes. However, the temperature dependence of a_T and τ^* scales not with the total free volume but with the relative change in free volume over the temperature range of interest. As shown in Figure 10b, the normalized free volume of **P-1** increases at a greater rate with increasing temperature than that of PX-1000 or PX-2000. This difference may be explained by the main chain flexibility of **P-1** due to incorporation of *m*-phenylene segments. As temperature increases above T_g, the rigid-rod character of PX-1000 and PX-2000 restricts free volume expansion to librations and rotations of the side groups around the main chain while the *m*-phenylene kink units in **P-1** allow for long range diffusive mobility and main chain segmental motion with a large swept volume. Since the intermolecular coupling parameter n varies only within experimental error as a function of molecular structure, an alternate explanation of the fragility of the polyphenylenes is necessary. The differences in the temperature dependence of relaxation times of the Poly-X resins can be explained in a straightforward manner by the relative change of free volume with temperature in each of the substituted poly(*p*-phenylenes).

IV. Conclusions

Poly(*p*-phenylene) resins containing benzoyl and 4-phenoxybenzoyl side groups display flexural moduli approaching 10 GPa and glass transition temperatures above 150 °C as well as low dielectric constants and low dielectric loss under ambient conditions. As shown by dynamic mechanical and expansion coefficient measurements, the T_g of these polymers varies with free volume. The 4-phenoxybenzoyl-substituted polyphenylene exhibits the lowest T_g and largest free volume but displays the highest intramolecular bond rotational barrier due the bulkiness of the side group. The temperature dependence of dielectric and viscoelastic relaxation times in these substituted polyphenylenes can be explained by simple free volume considerations. The "fragility" or temperature sensitivity of relaxation times correlates not with total free volume but with the relative change in free volume with respect to the free volume at T_g.

Acknowledgment. We thank Drs. John Bendler and Andrea Schmitz of General Electric Corp. for their computer program for calculating KWW relaxation spectra and Professor Paul Lahti for the use of his Silicon Graphics workstation. This work was supported by Air Force Office of Scientific Research Grant 94-01.

References and Notes

(1) Rehahn, M.; Schlüter, A. D.; Wegner, G.; Feast, W. J. *Polymer* **1989**, *30*, 1054.

(2) Philips, R. W.; Sheares, V. V.; Samulski, E. T.; DeSimmone, J. M. *Polym. Prepr. (Am. Chem. Soc., Div. Polym. Chem.)* **1994**, *35*, 367.

(3) Wang, G. Y.; Quirk, R. P. *Polym. Prepr. (Am. Chem. Soc., Div. Polym. Chem.)* **1994**, *35*, 503.

(4) Bae, J.; Zhao, M. Y.; Hill, D. H.; Percec, V. *Proc. 35th IUPAC Macro. Symp.* **1994**, 139.

(5) Marrocco, M. L.; Gagné, R. R.; Trimmer, M. S. U.S. Patent 5,227,457.

(6) Gagné, R. R.; Harding, S.; Marrocco, M.; Trimmer, M. S.; Wang, Y. *Polymer Prepr. (Jpn.)* **1993**, *42* (1), 138.

(7) Marrocco, M. L.; Trimmer, M. S.; Hsu, L.-C.; Gagné, R. R. *Proc. Int. SAMPE Symp.* **1994**, *39*, 1063.

(8) Plazek, D. J.; Ngai, K. L. *Macromolecules* **1991**, *24*, 1222.

(9) (a) Roland, C. M.; Ngai, K. L. *Macromolecules* **1991**, *24*, 5315. (b) *Macromolecules* **1992**, *25*, 1844 (correction).

(10) Ngai, K. L.; Roland, C. M. *Macromolecules* **1993**, *26*, 6824.

(11) Kaye, W.; McDaniel, J. B. *Appl. Opt.* **1974**, *13*, 1934.

(12) Weiss, G. H.; Bendler, J. T.; Dishon, M. *J. Chem. Phys.* **1985**, *83*, 1424.

(13) Weiss, G. H.; Dishon, M.; Long, A. M.; Bendler, J. T.; Jones, A. A.; Inglefield, P. T.; Bandis, A. *Polymer* **1994**, *35*, 1880.

(14) McClellan, A. L. *Tables of Experimental Dipole Moments*; W. H. Freeman & Co.: San Francisco, 1963.

(15) Williams, M. L.; Landel, R. F.; Ferry, J. D. *J. Am. Chem. Soc.* **1955**, *77*, 3701.

(16) Doolittle, A. K. *J. Appl. Phys.* **1952**, *23*, 418.

(17) Vogel, H. *Phys. Z.* **1921**, *22*, 645.

(18) Fulcher, G. S. *J. Am. Chem. Soc.* **1925**, *8*, 339.

(19) Ngai, K. L.; Mashimo, S.; Fytas, G. *Macromolecules* **1988**, *21*, 3030.

(20) Zhong, Z. Z.; Schuele, D. E.; Smith, S. W.; Gordon, W. L. *Macromolecules* **1993**, *26*, 6403.

(21) Roland, C. M.; Santangelo, P. G.; Ngai, K. L.; Meier, G. *Macromolecules* **1993**, *26*, 6164.

(22) Santangelo, P. G.; Ngai, K. L.; Roland, C. M. *Macromolecules* **1994**, *27*, 3859.

(23) Ferry, J. D. *Viscoelastic Properties of Polymers*, 3rd ed.; Wiley: New York, 1980; pp 287 & 289.

(24) Matsuoka, S. *Relaxation Phenomena in Polymers*; Hanser: New York, 1992.

(25) Angell, C. A. *J. Non-Cryst. Solids* **1991**, *131–133*, 13.

(26) Williams, G.; Watts, D. C. *Trans. Faraday Soc.* **1970**, *66*, 2503.

(27) Frölich, H. *Theory of Dielectrics*; Oxford University Press: London, 1958.

(28) Bueche, F. *J. Chem. Phys.* **1953**, *21*, 1850.

(29) Fox, T. G.; Flory, P. J. *J. Appl. Phys.* **1950**, *21*, 581.

(30) Fox, T. G.; Flory, P. J. *J. Polym. Sci.* **1954**, *14*, 315.

MA945019Z